

## **Supplement 1: Methods**

### **Tissue lipid analyses.**

Lipid extraction was performed according to the method of Matyash *et al.* (1). In brief, 25 mg of frozen liver or muscle tissue were added to 2 mL tough tubes (Geneworks, Hindmarsh, SA, Australia) on dry ice and stored at -80°C. An aliquot of 200 µL of methanol containing 0.01% butylated hydroxytoluene, 2 nmoles of ceramide (17:0) and 10 nmoles of DAG (17:0/17:0) was added to each tube. Samples were homogenised on a FastPrep-24 (MP Biomedical, Seven Hills, NSW, Australia) at 6 m/s for 40 sec. Beads were washed with 200 µL methanol and the wash added to homogenate. Aliquots of 300 µL were removed to 2 mL microcentrifuge tubes (Eppendorf, North Ryde, NSW, Australia), 1 mL of methyl-tert butyl ether was added and samples were vortexed for 1 hr at 4°C. An addition of 250 µL of 150 mM ammonium acetate was added to induce phase separation. Tubes were vortexed and spun at 2000 g for 5 minutes to complete phase separation. Approximately 800 µL of the upper organic layer was removed to a new 2 mL glass vial, dried under a stream of nitrogen at 37°C, resuspended in 500 µL methanol:chloroform (2:1 v/v) and stored at -20°C until analysis. Samples were diluted 200-fold into methanol:chloroform (2:1 v/v) containing 5 mM ammonium acetate prior to mass spectrometric analysis.

Mass spectra were acquired using a TriVersa Nanomate<sup>®</sup> (Advion, Ithaca, NY, USA) coupled to a hybrid linear ion trap-triple quadrupole mass spectrometer (QTRAP<sup>®</sup> 5500, ABSCIEX, Foster City, CA, USA). The pipette tip in the TriVersa Nanomate<sup>®</sup> aspirated 10 µL of extract from a sealed 96-well plate and delivered extract into the mass spectrometer via a nano-ESI chip with an orifice diameter of 4.1 µM. The delivery gas was N<sub>2</sub> at a pressure of 0.4 psi and spray voltage of 1.15 kV. Ceramide molecular lipids were analysed by precursor-ion scanning for protonated dehydrated sphingosine at  $m/z$  264.3. Diacylglycerol molecular lipids were analysed by multiple neutral-loss scanning for ammoniated fatty acids. Experimental conditions for acquisition were a declustering potential of 100 V, entrance potential of 10 V, CID energy of 35 eV and a scan rate of 200  $m/z$  units.s<sup>-1</sup>. Mass spectra were averaged over 50 scans. Data were analyzed with LipidView<sup>®</sup> (ABSCIEX) version 1.1, including smoothing, identification, de-isotoping, and isotope correction. Quantification was achieved in LipidView<sup>®</sup> by comparison of the peak area of individual lipids to their class-specific internal standards after isotope correction.

1. Matyash V, Liebisch G, Kurzchalia TV, Shevchenko A, Schwudke D: Lipid extraction by methyl-tert-butyl ether for high-throughput lipidomics. *Journal of Lipid Research* 49:1137-1146, 2008

### **SDS-PAGE and immunoblotting (cont.).**

Briefly, primary antibody incubations were carried out at a dilution of 1:1000 for 3 hours at room temperature or overnight at 4 °C. Equal loading of protein between lanes was confirmed by subsequent skeletal actin (for muscle) and 14-3-3 (for liver) immunoblots. After incubation with horseradish peroxidase-conjugated sheep anti-mouse or donkey anti-rabbit (1:10000; Jackson ImmunoResearch, West Grove, PA, USA) antibody for 1.5 hrs at

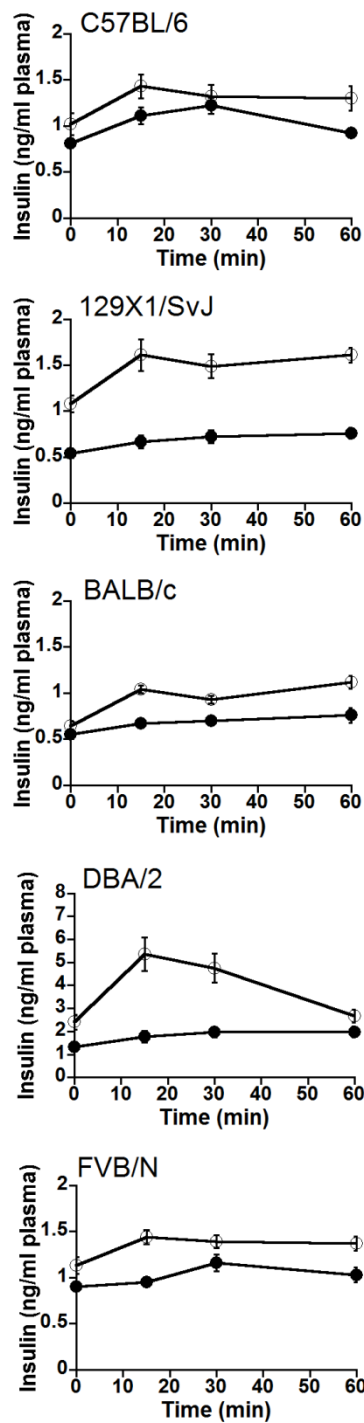
room temperature, immunodetection was performed by chemiluminescence (PerkinElmer, Wellesley, MA, USA or Millipore, Billerica, MA, USA).

Fatty acid transport protein (FATP) 2 and 14-3-3 antibodies were purchased from Santa Cruz Biotechnology (Santa Cruz, CA, USA); carnitine palmitoyltransferase-1 (CPT1) from Alpha Diagnostic International (San Antonio, TX, USA);  $\text{I}\kappa\beta$ , phospho and total  $\text{IKK}\alpha/\beta$ , phospho (Thr183/Tyr185, 9251)- and total JNK (9252), as well as fatty acid synthase (FAS), stearoyl-CoA desaturase (SCD-1) and acetyl-CoA carboxylase (ACC) from Cell Signaling Technology (Danvers, MA, USA); peroxisome proliferator-activated receptor (PPAR)- $\gamma$  coactivator (PGC)-1 $\alpha$  from Chemicon International (Temecula, CA, USA); pyruvate dehydrogenase kinase 4 (PDK4; kind gift of Robert A. Harris, Indiana University, IN) ; uncoupling protein 3 (UCP3) from Affinity Bioreagents (Golden, CO, USA); fatty acid transport (FATP) protein 4 and skeletal muscle actin from Abcam (Cambridge, USA); cytochrome oxidase (complex IV) subunit 1 from Invitrogen (Victoria, Australia); and an antibody cocktail that recognizes several subunits of the mitochondrial respiratory chain (MS601) from Mitosciences (Eugene, OR, USA).

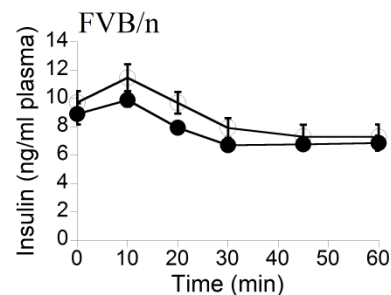
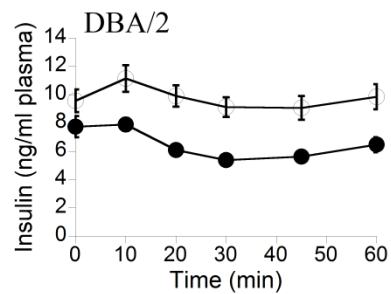
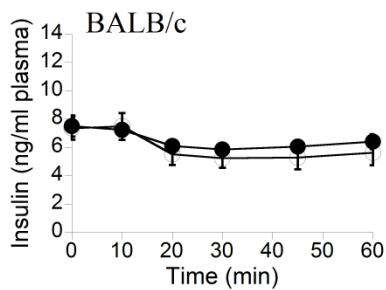
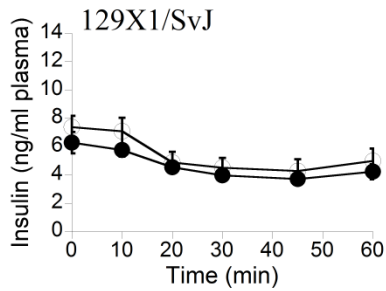
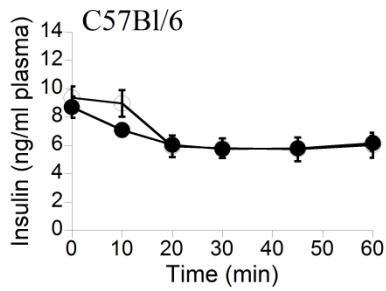
## **Supplement 2: Results**

**Supplementary Table 1:** Adipose tissue inflammation primer sequences.

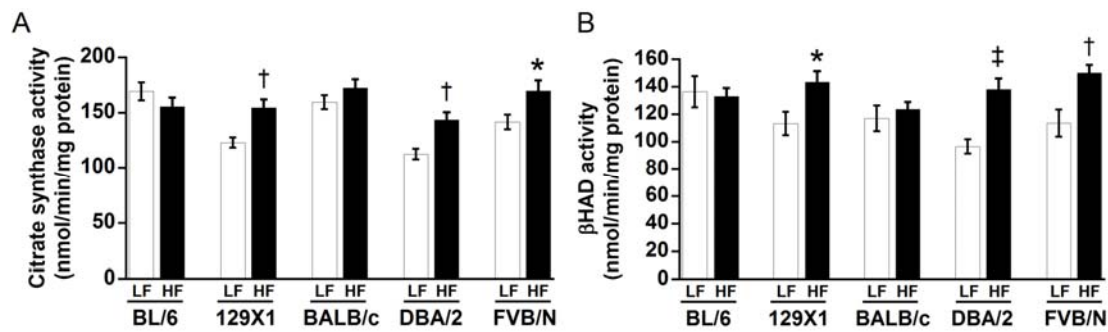
<b>Inflammation Marker</b>	<b>Primer Sequence</b>
<b>F4/80</b>	Forward: CCTGGACGAATCCTGTGAAG Reverse: GGTGGGACCACAGAGAGTTG
<b>CD11c<sup>+</sup></b>	Forward: ATGGAGCCTCAAGACAGGAC Reverse: GGATCTGGGATGCTGAAATC
<b>CD68</b>	Forward: GACCTACATCAGAGCCCGAGT Reverse: CGCCATGAATGTCCACTG
<b>TNF<math>\alpha</math></b>	Forward: CCCCTTTACTCTGACCCCTTTATTG Reverse: AACCTGACCACTCTCCCTTTGC
<b>MCP-1</b>	Forward: CCACTCACCTGCTGCTACTCATTC Reverse: TCTGGACCCATTCCTTCTTGG
<b>IL-6</b>	Forward: CAAGAGACTTCCATCCAGTTGCC Reverse: CATTTCCACGATTTCCCAGAGAA
<b>HPRT</b>	Forward: TCCTCCTCAGACCGCTTTT Reverse: CCTGGTTCATCATCGCTAATC



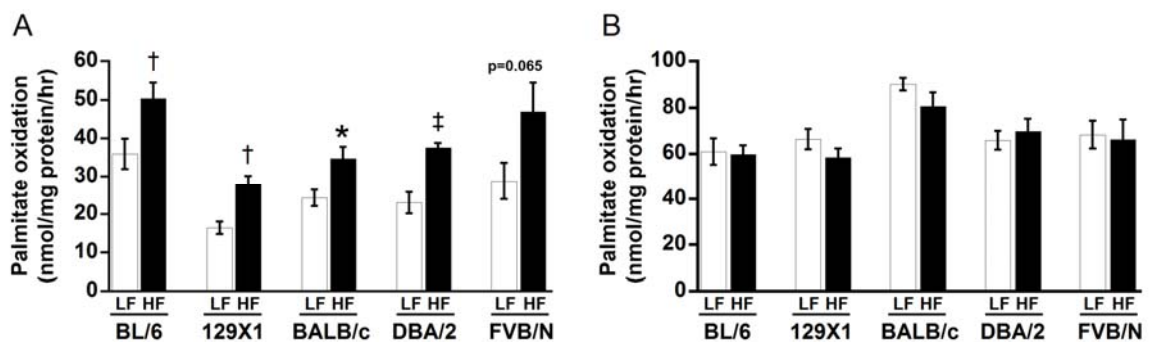
Supplementary Figure 1: Insulin levels during the intraperitoneal glucose tolerance test in low-fat (LF) and high-fat (HF) fed mice. Glucose (2g/kg) was injected at the 0 time point and plasma insulin levels were monitored for 60min post-injection. black dots = LF mice, white dots = HF mice; n = 6-8 for each strain and diet group.



Supplementary Figure 2: Insulin (0.75U/kg) was injected at the 0 time point and blood glucose levels were monitored for 90min post-injection. black dots = LF mice, white dots = HF mice; end point body weight  $p < 0.0001$  for BL6, 129X1, DBA/2 and FVB/N;  $n = 6-8$  for each strain and diet group.



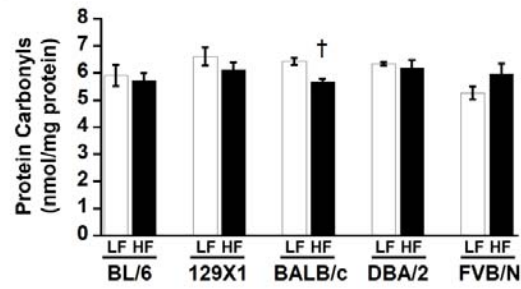
Supplementary Figure 3: Markers of mitochondrial content and metabolism. Liver citrate synthase (A) and  $\beta$ -hydroxyacyl CoA dehydrogenase ( $\beta$ HAD) (B) activity in low-fat (LF) and high-fat (HF) fed mice; white bars = LF mice, black bars = HF mice; \*  $p < 0.05$ , †  $p < 0.01$ ;  $n = 6-8$  for each strain and diet group.



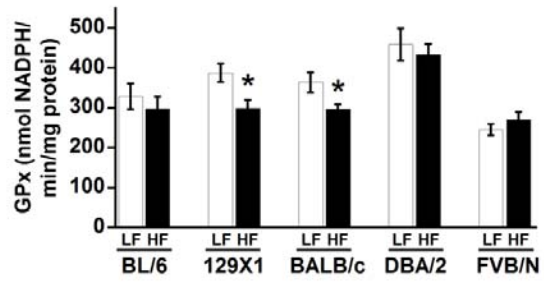
Supplementary Figure 4: Palmitate oxidation in muscle (A) and liver (B) homogenates, measured in low-fat (LF) and high-fat (HF) fed mice; white bars = LF mice, black bars = HF mice; \* when  $p < 0.05$ , †  $p < 0.01$ ; ‡  $p < 0.0001$ ;  $n = 6-8$  for each strain and diet group.

## Muscle

A

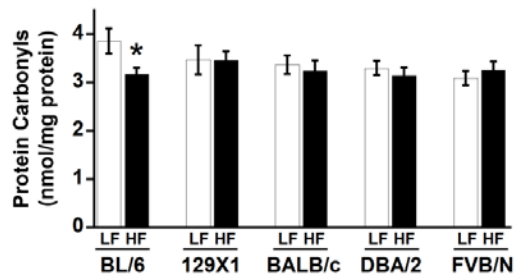


B

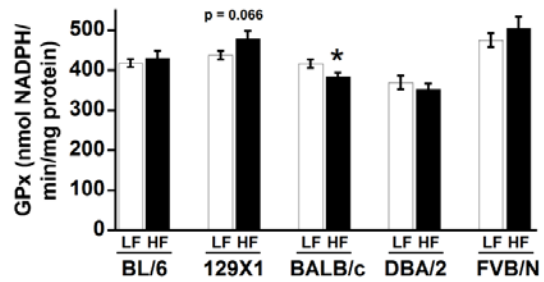


## Liver

C



D



Supplementary Figure 5: Markers of oxidative damage and antioxidant protection. Protein carbonyl (LOOH) (A and C) and glutathione peroxidase (GPx) (B and D) were measured in low-fat (LF) and high-fat (HF) fed mice; white bars = LF mice, black bars = HF mice; \*  $p < 0.05$ , <sup>†</sup>  $p < 0.01$ ;  $n = 6-8$  for each strain and diet group.